N.; Monnerie, L.; Bokobza, L. *Macromolecules* **1982**, *15*, 64.
(11) Smit, K. J.; Sakurovs, R.; Ghiggino, K. P. *Eur. Polym. J.* **1983**, *19*, 49.
(12) Beavan, S. W.; Hargreaves, J. S.; Phillips, D. *Adv. Photochem.* **1979**, *11*, 207.
(13) Rutherford, H.; Soutar, I. *J. Polym. Sci., Polym. Phys. Ed.* **1977**, *15*, 2213.
(14) Somersall, A. C.; Dan, E.; Guillet, J. E. *Macromolecules* **1974**, *7*, 233.
(15) Goldenberg, M.; Emert, J.; Morawetz, H. *J. Am. Chem. Soc.* **1978**, *100*, 7171.
(16) Aspler, J. S.; Guillet, J. E. *Macromolecules* **1979**, *12*, 1082.
(17) Salom, C.; Hernández-Fuentes, I., unpublished results.
(18) Tanabe, Y. *J. Polym. Sci., Polym. Phys. Ed.* **1985**, *23*, 601.

Glass Transition and Melting Behavior of Poly(oxy-2,6-dimethyl-1,4-phenylene)

Stephen Z. D. Cheng* and Bernhard Wunderlich

Department of Chemistry, Rensselaer Polytechnic Institute, Troy, New York 12181-3590.
Received September 26, 1986

ABSTRACT: Thermal analysis of amorphous and semicrystalline poly(oxy-2,6-dimethyl-1,4-phenylene) (PPO) has been carried out from 220 to 580 K. In the solid state, glassy and semicrystalline PPO were shown to have the same heat capacity up to 420 K (±1.6%, 25 samples, 30 measurements). Liquid PPO follows a linear heat capacity dependence (400–580 K, ±1.5%, 25 samples, 30 runs). Both sets of new data agree with the "Athas recommended data (1985) and (1980)", respectively so that no new recommendation is made (deviation from the recommended solid and liquid data: −0.3% ± 0.5% and +0.25% ± 0.003%, respectively). Based on the confirmed heat capacities, a detailed glass and melting transition study has been performed. Crystals of PPO are, as is well-known, rather imperfect, and it is shown here that they are coupled to a large fraction of "rigid-amorphous" polymer, which, in turn, governs the crystal annealing. Hysteresis at the glass transition, low heat capacity below the glass transition of as-polymerized samples, and decrease in crystallinity with increase in crystal perfection on annealing below the melting temperature are described and discussed.

Introduction

Poly(oxy-2,6-dimethyl-1,4-phenylene) (PPO) has been a commercially important polymer since its discovery over 20 years ago.[1,2] Thermal properties of the homopolymer have first been measured by Karasz et al.,[3] using adiabatic calorimetry.

From 80 to 420 K, it was shown that semicrystalline and amorphous solid PPO had within experimental error identical heat capacities, C_p. Since then the measurements have been repeated and fitted to the vibrational spectrum of solid PPO.[4-6] The group vibrations were approximated by single frequencies and box distributions, while the five skeletal vibrations were described by the $\theta_1 = 564$ K and $\theta_3 = 40$ K temperatures in a Tarasov equation.[4]

Above the glass transition temperature, T_g, at 482 K, the liquid amorphous PPO has a higher heat capacity. The increase in ΔC_p at T_g for amorphous PPO was first reported[3,6] to be 28.8 J/(K mol), close to the present Athas recommended value of 31.9 J/(K mol).[4,5] A suggested absence of the glass transition for a 25% crystalline sample[3] (by X-ray) was surprising and will be shown below to be caused by the existence of "rigid-amorphous" PPO. A large number of additional C_p measurements for solid and liquid PPO which are in agreement with the prior work will be presented in this research report.

The semicrystalline PPO analyzed by Karasz et al.[3] showed a somewhat smaller heat capacity in the temperature range from 420 to 482 K than the expected one for solids. It will be shown here that this is a repeatable phenomenon, although short-time annealing will increase the heat capacity to the expected value. An alternative explanation to the original suggestion of some crystallization below T_g will be offered.

A melting transition endotherm at 510 K was seen for the semicrystalline PPO.[3] From the end of melting, a first estimate of the equilibrium melting temperature was made to be 535 K. Such low melting temperature, T_m, leads to the unusually high T_g/T_m ratio of 0.9 (attributed originally to a low entropy of fusion). More recent extrapolations[7-9] led to estimates ranging from 563 to 583 K for the equilibrium melting temperature, $T_m°$. Heats of fusion, $\Delta h_f°$, were difficult to assess since PPO crystallizes frequently with incorporation of solvent molecules into the crystal.[9,10] Values of 3–10 kJ/mol have been reported (extrapolated to 100% crystallinity).[3,7,11,12] For the present work it was decided that the most recent values of van den Berg and co-workers[9] are perhaps most reliable ($T_m° = \sim 580$ K, $\Delta h_f° = 5.95$ kJ/mol).

A wide application of PPO involves compatible blends, in particular with polystyrene.[2] The thermal properties of isotactic polystyrene blended with PPO have been reported as a eutectic system.[13-16] By use of mainly mechanical analysis, blends with nylon 66 have been studied.[17] Effects of bromine[18,19] and phosphonyl[19] substitution on the phenylene group on the glass transition have also been investigated by thermal analysis.

Solution crystallization of PPO was studied,[9,20] and the morphology of the resulting crystals has been reported.[10] It is generally accepted that solvent molecules are incorporated into the PPO crystal.[7] Removal of the solvent on drying leaves severely distorted and defect crystals.[7,10] Melt crystallization, in contrast, has received less attention.[8] It was not possible to crystalline PPO melt in the narrow temperature range between T_g and T_m in isothermal experiments of 8-h duration. It is reported, however,[8] that nucleating agents such as anthraquinone or 2-mercaptobenzimidazole can cause crystallization with Avrami exponents of 1.6. Exposure to solvent vapors, such as 2-butanone, also leads to crystallization.[10]

Compared to other phenylene-containing macromolecules such as poly(ethylene terephthalate),[21] poly(oxy-1,4-phenyleneoxy-1,4-phenylenecarbonyl-1,4-phenylene) (PEEK),[22] and poly(thio-1,4-phenylene) (PPS),[23] the thermal properties of PPO were less well understood. The

0024-9297/87/2220-1630$01.50/0

present work will show that some of the thermal properties of PPO such as the interplay between rigid amorphous and crystals may be unique.

Experimental Section

Materials and Samples. The PPO for this research was kindly provided by General Electric Company, Noryl Products Department, Selkirk, NY (courtesy of R. C. Bopp), as the usual as-produced powder. The intrinsic viscosity of this PPO in $CHCl_3$ at 303.2 K was 0.46 dL/g. The molecular masses of the PPO sample were reported to us to be M_w = 44 000 and M_n = 19 000. DSC samples of the PPO were enclosed in aluminum pans. The sample weight was above 15 mg to obtain heat capacity measurements of reasonable accuracy. Sample and pan weights were recorded to ±1 μg.

Equipment and Experiments. A Perkin-Elmer DSC 2 was used for thermal analysis of all PPO samples. The analog output was fed after conversion to frequency into an IBM-PC LMS DSC data station. There are at present 12 data points recorded per degrees kelvin. Both, temperature and heat capacity calibrations were performed following the standard procedures (*n*-heptane, *n*-octane, *n*-decane, *n*-dodecane, naphthalene, benzoic acid, indium, tin, lead, and zinc melting for temperature and sapphire for heat capacity calibration[24]). For the measurements of heat capacity, the base lines of the empty pan and sapphire reference were measured and compared to the heat flow measurements of the PPO samples. The standard heating rate was 10 K/min. All runs were made in a dry nitrogen atmosphere. The calorimeter is shielded in the drybox attachment of the Perkin-Elmer DSC 2. The calorimeter room is held at ±1 °F.

Three temperature ranges were used for measurement: 220–350, 325–420, and 400–580 K. The first two are well below the glass transition temperature region, and the last one involves both glass transition and melting transition. If the PPO samples were heated above melting (580 K), held 2 min, and then cooled below T_g, glassy amorphous PPO samples were obtained. Different cooling rates were used to study the hysteresis effect at the glass transisition of amorphous PPO (−0.31 K/min to quenching in liquid N_2). Even at the slow cooling rates there is no interference due to crystallization of PPO once the crystals had been totally molten.

The isothermal annealing experiments were carried out in the temperature range from 493.2 to 505.2 K. The as-received samples were heated to the fixed annealing temperature at a rate of 10 K/min from below T_g, and different annealing times were chosen. Then, the samples were cooled again to below T_g and reheated for thermal analysis (both at 10 K/min). Slower cooling rates to enhance the hysteresis effect were not possible because of additional annealing on cooling.

Some Definitions. Three terms used in this paper are in need of definition: rigid fraction, f_r; crystallinity, w_c, and rigid-amorphous fraction.

The rigid fraction is defined as

$$f_r = 1 - \frac{\Delta C_p(\mathrm{m})}{\Delta C_p(\mathrm{a})} \tag{1}$$

where ΔC_p(m) and ΔC_p(a) are the measured heat capacity increases at the glass transition temperature, T_g, for semicrystalline and totally amorphous PPO, respectively. The rigid fraction is thus the fraction of the polymer that does not contribute to ΔC_p at T_g.

The definition of crystallinity is, as usual,

$$w^c = \frac{\Delta h_f(\mathrm{m})}{\Delta h_f(\mathrm{c})} \tag{2}$$

where Δh_f(m) and Δh_f(c) are the heats of fusion for the (measured) semicrystalline sample and for 100% crystalline PPO, respectively.

Based on eq 1 and 2 the rigid-amorphous fraction can easily be determined as $f_r - w^c$. The first detailed description of a rigid-amorphous fraction in semicrystalline polymers is given in ref 25.

The glass transition region is characterized by five temperatures. The first perceptible beginning of the glass transition, T_b, is judged by the first increase in heat capacity from that of the solid state (glassy or crystalline). The extrapolated beginning and end of the glass transition, T_1 and T_2, are indicative of the broadness of the major portion of the glass transition. The glass transition temperature, T_g, is chosen at half-devitrification when judged by heat capacity increase. Finally, T_e, the end of glass transition, is reached when the heat capacity reaches the liquid heat capacity. In case of hysteresis at the glass transition, its peak temperature is recorded. The endothermic peak area above the liquid base line was measured for the discussion of hysteresis.

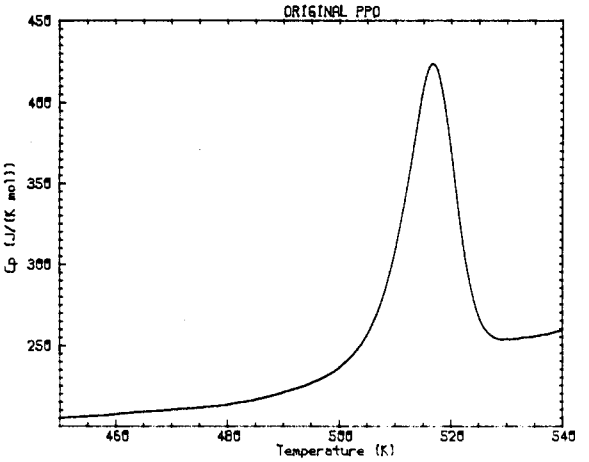

Figure 1. DSC melting trace of PPO, as received. The crystallinity is 28% ± 3%. The melting peak temperature is 517 K, and the end melting temperature is 527 K. The heating rate is 10 K/min.

For the melting peak, two characteristic temperatures are considered: the peak (maximum) temperature, T_m(P), and the end temperature, T_m(e). T_m(e) was usually determined by the extrapolated onset point between the liquid base line and ending endothermic peak line where the heat capacity decreases.

Results

Characteristics of the Original PPO Samples. The PPO samples provided by the G.E. Company (powder, as polymerized and precipitated) have been characterized as received by DSC as shown in Figure 1. As reported earlier,[3] there is no obvious glass transition. Furthermore, starting at 440 K, the heat capacity shown in Figure 1 is somewhat lower than the calculated solid heat capacity based on vibrational spectra:[4] −1.4% at 450 K; −1.9% at 460 K; −2.2% at 470 K; and −2.3% at 480 K. An estimate of this overall exothermic heat effect is 240 J/mol from 440 to 480 K. The crystallinity of this PPO sample was 28% ± 3% derived from its heat of fusion. The peak melting temperature was 517 K, and the end of the melting temperature was 527 K.

Crystallinities determined by X-ray diffraction on similar PPO samples were reported also to be in the range of 30%.[10] A more detailed study of the annealing behavior using X-ray diffraction has been initiated in our laboratory. In general the diffraction paterns are very broad and ill defined, indicative of poor and small crystals. Typical values[10] for the average crystal dimensions that fit the low-angle X-ray scattering data were reported to be $\bar{x}_c$ = 3–4 nm, $\bar{x}_a$ = ~10 nm, and $\bar{x}_b$ = 1 nm.

Solid-State Heat Capacities of PPO. In the ATHAS data bank (1985),[4] the solid heat capacity of PPO has been reported from 0 K to T_m°. These data are based on earlier calorimetry,[3,6] empirical smoothing,[5] and links with calculated heat capacities based on the vibrational spectrum of PPO.[4] In the present work, measurements on solid PPO were carried out from 220 to 480 K for the solid. Both amorphous and semicrystalline samples were measured. Their heat capacities below T_g agree to better than ±1% in this temperature range. As for most polymers, and as

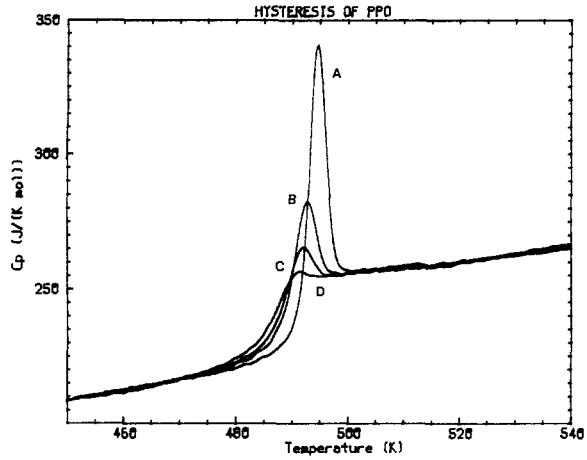

Figure 2. Hysteresis study of amorphous PPO cooled at different cooling rates through the glass transition. From right to left: (A) −0.31 K/min; (B) −2.5 K/min; (C) −10 K/min; and (D) quenched in liquid N_2. The heating rate is 10 K/min.

reported before,[4] there is a crystallinity or rigid-fraction independence of C_p below T_g. The heat capacities measured in the present research were fitted to the following equation (rms deviation of the averages of C_p at each temperature: ±0.2%):

$$C_p = \exp[-0.13222(\ln T)^3 + 2.2301(\ln T)^2 - 1.1681(\ln T) + 23.614] \quad (3)$$

[in J/(K mol), 30 runs on 25 samples, 220–460 K, ±1.6% agreement at the various temperatures between the 30 runs]. Equation 3 agrees with the calculated heat capacities of ref 4 with a deviation of −0.3% ± 0.5%, so that it was not felt necessary to revise the ATHAS recommended data (1985).

Liquid Heat Capacities and Glass Transition of Amorphous PPO. Since no crystallization can be found during cooling after the PPO samples were heated above 580 K (see below), the liquid heat capacities of PPO can be measured directly starting from T_g. The data can be expressed by (rms deviation of the averages of C_p at each temperature: ±0.5%)

$$C_p = 0.2282T + 141.6 \quad (4)$$

[in J/(K mol), 30 runs on 25 samples, 400–580 K, ±1.5% agreement at the various temperatures between the 30 runs].

Equation 4 agrees closely with the ATHAS recommended data for liquid PPO of 1980[5] (+0.250 ± 0.003%) so that it was not felt necessary to revise these earlier data. The new data give strong support to the earlier adiabatic calorimetry.[3] A detailed description of integral thermodynamic functions will be given at a later time.[26]

The glass transition temperature of the amorphous samples was found to be 484 K after correction of hysteresis effect (see below), and ΔC_p at 484 K was measured to be 32 J/(K mol). It fits the calculation data from the recommended data well [31.9 J(K mol)]. Typical DSC traces of amorphous PPO in the glass transition region are shown in Figure 2.

Hysteresis in the T_g Region. Hysteresis effects at the glass transition are introduced by thermal history of the samples (either varying cooling rates through T_g or annealing close to, but below, T_g). Figure 2 shows that increasingly endothermic hysteresis peaks on heating are found with decreasing cooling rates on prior cooling through T_g. At a cooling rate of 0.31 K/min, the peak area Δh = 240 J/mol, curve A in Figure 2. However, a hysteresis peak can still be seen in the case of a cooling rate

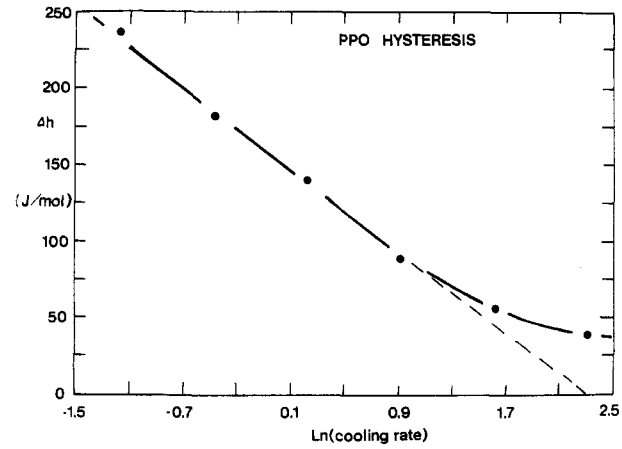

Figure 3. Relationship between the enthalpy of the hysteresis peak and the logarithm of the cooling rate for amorphous PPO. The heating rate is 10 K/min (ln 10 = 2.30).

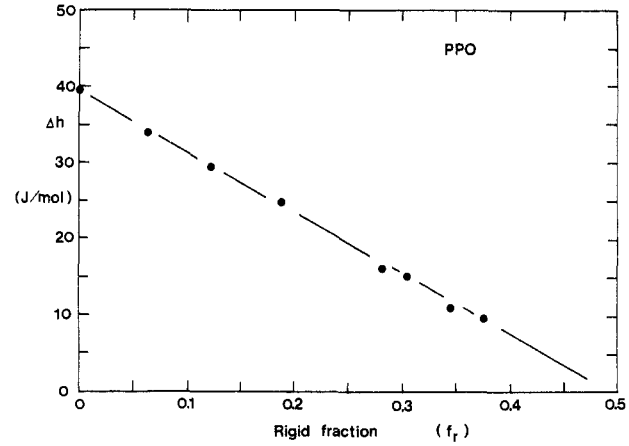

Figure 4. Relationship between the enthalpy of the hysteresis peak and the rigid fraction of semicrystalline PPO. Both prior cooling and heating rates are 10 K/min.

10 K/min (Δh = 39 J/mol, curve C in Figure 2). Moreover, even the quenched PPO sample shows a small hysteresis peak (Δh = 7.5 J/mol, curve D in Figure 2). On the other hand, there is no indication of an exothermic hysteresis peak below T_g for the quenched sample as one might expect (three quenched PPO samples showed repeatable results). Figure 3 indicates that there exists a linear relationship between Δh of the endothermic hysteresis peak (above the liquid heat capacity base line) and the logarithm of the prior cooling rate only in the 0.31–2.5 K/min range. Starting from a cooling rate of 5 K/min, a higher Δh is observed then expected by linear extrapolation from the slower cooling rates. The extrapolation of the straight line to Δh = 0 leads to a cooling rate of 10 K/min, the heating rate used, as is expected from comparison with other polymers.

For semicrystalline PPO, the hysteresis peak can also be observed (see below, Figures 6–10). The hysteresis effect of semicrystalline PPO is proportional to $(1 - f_r)$, but the observed hysteresis peak is smaller than expected from the remaining amorphous PPO as shown in Figure 4. Zero hysteresis is reached at 0.5 rigid fraction at cooling and heating rates of 10 K/min (curve C in Figure 2, for amorphous PPO Δh = 39 J/mol).

Glass Transition of Semicrystalline PPO. From Figure 1, one can find that there is no easily recognizable glass transition below PPO crystal melting, even though only about 30% crystallinity exists in these samples. However, a glass transition does appear after annealing experiments are carried out. A quantitative analysis shows

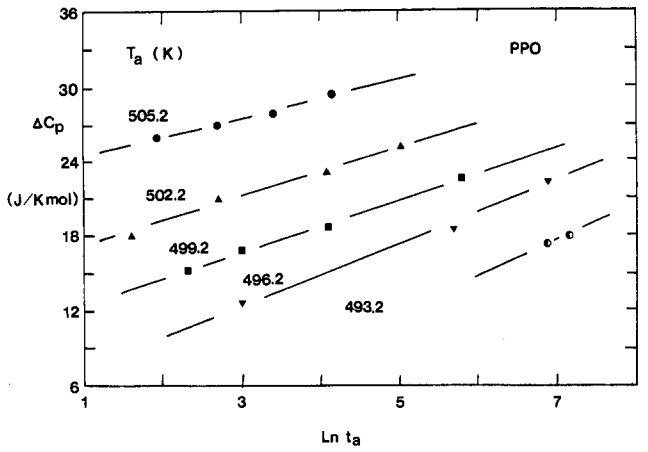

Figure 5. Relationship between the heat capacity increase at T_g and the logarithm of annealing time at different annealing temperatures. The heating rate is 10 K/min for all samples.

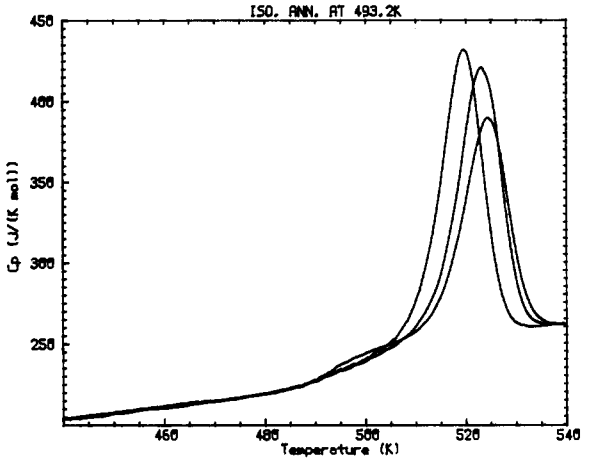

Figure 6. DSC melting traces after annealing at 493.2 K at three different times (from left to right): 15, 60, and 960 min. Cooled to 400 K after annealing at 10 K/min and then reheated at 10 K/min.

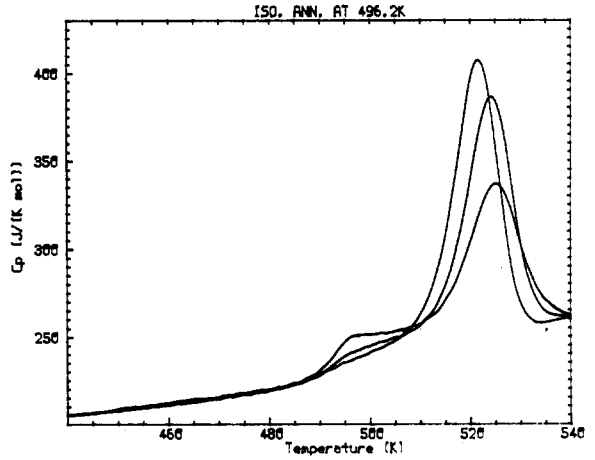

Figure 7. DSC melting traces after annealing at 496.2 K at three different times (from left to left): 20, 300, and 990 min. (For measuring conditions, see Figure 6.)

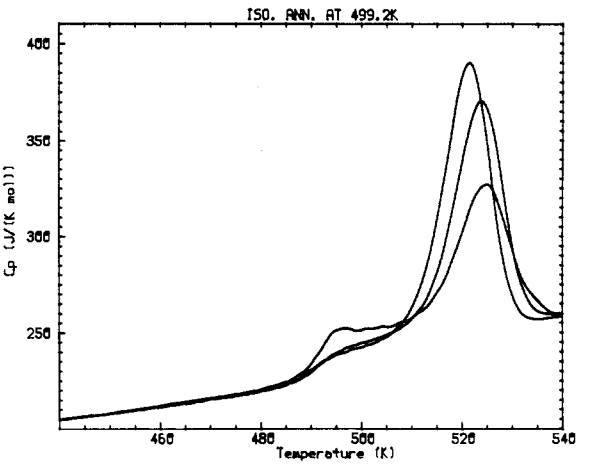

Figure 8. DSC melting traces after annealing at 499.2 K at three different times (from left to right): 10, 60, and 330 min. (For measuring conditions, see Figure 6.)

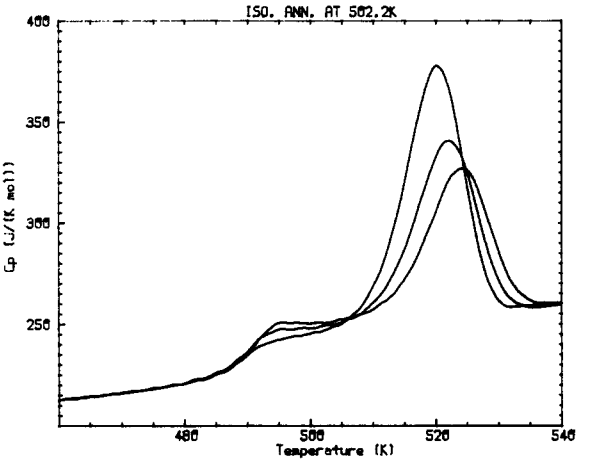

Figure 9. DSC melting traces after annealing at 502.2 K at three different times (from left to right): 5, 15, and 60 min. (For measuring conditions, see Figure 6.)

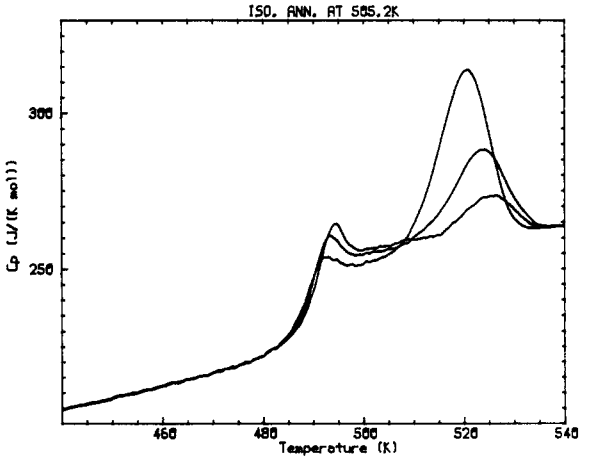

Figure 10. DSC melting traces after annealing at 505.2 K at three different times (from left to right): 7, 15, and 65 min. (For measuring conditions, see Figure 6.)

that the glass transition temperature, T_g, heat capacity increases at T_g, ΔC_p, and the main broadness of the glass transition region is annealing temperature and time dependent. In Table I these parametters of the glass transition are listed. The end of the glass transition at T_e, and in some cases also T_2, cannot be determined since they merge with the melting peak. One can find, from Table I, that higher annealing temperatures and longer annealing times give lower glass transition temperatures and larger heat capacity increases at T_g. Figure 5 shows the relationship between the heat capacity increase at T_g at different annealing temperatures and times.

Melting Temperatures of Semicrystalline PPO. Figures 6–10 show DSC melting traces of the originally semicrystalline PPO (see Figure 1) after annealing at different temperatures and varying times. One can find

Table I
Thermal Properties of the As-Received PPO in the Glass Transition Region Measured by Heating after Annealing for Time t_a at Temperature T_a

	T_a, K	t_a, min	T_b, K	T_1, K	T_g, K	T_2, K	ΔT_1, K	ΔC_p, J/(K mol)
Am. PPO			460.0	480.0	483.0	488.0	8.0	32
A								
	493.2	15	460.0	(?)[a]	(?)	(?)	(?)	(?)
	493.2	60	460.0	(?)	(?)	(?)	(?)	(?)
	493.2	960	460.0	486.0	495.0	(?)	(?)	17.4
	493.2	1200	460.0	486.0	495.0	(?)	(?)	18.5
B								
	496.2	20	460.0	485.0	494.0	(?)	(?)	12.7
	496.2	300	460.0	485.0	492.5	(?)	(?)	18.5
	496.2	990	460.0	484.0	492.0	(?)	(?)	22.3
C								
	499.2	10	460.0	484.5	491.0	497.5	13.0	15.4
	499.2	20	460.0	484.0	490.5	496.5	12.5	16.8
	499.2	60	460.0	483.0	489.0	494.5	11.5	18.6
	499.2	330	460.0	483.0	488.5	493.0	10.0	22.6
D								
	502.2	5	460.0	483.0	489.0	493.5	10.5	18.0
	502.2	15	460.0	483.0	488.5	493.0	10.0	21.0
	502.2	60	460.0	482.5	488.0	492.5	10.0	23.0
	502.2	150	460.0	482.0	487.0	491.5	9.5	25.0
E								
	505.2	7	460.0	481.5	485.0	491.0	9.5	26.0
	505.2	15	460.0	481.5	484.8	491.0	9.5	27.0
	505.2	30	460.0	481.0	484.5	490.0	9.0	28.0
	505.2	65	460.0	481.0	484.5	490.0	9.0	29.4

[a] (?) = value cannot be determined because of overlap with melting.

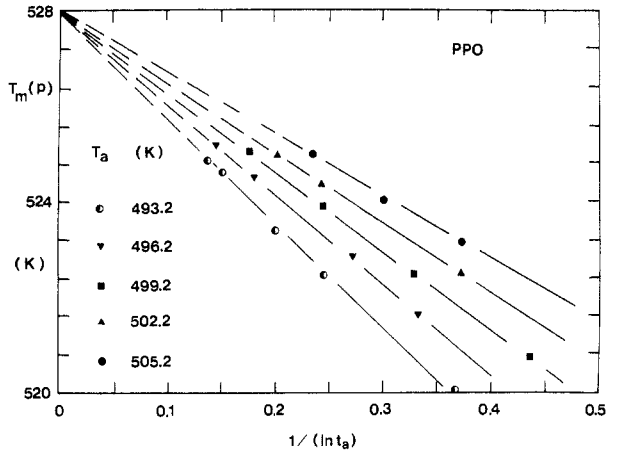

Figure 11. Relationship betwen T_m(p) and $[\ln t_a]^{-1}$ at five different annealing temperatures. The intersection of those five curves is at 528 K.

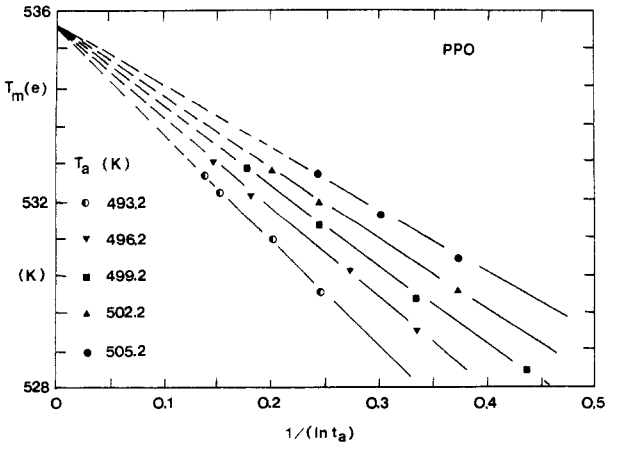

Figure 12. Relationship between T_m(e) and $[\ln t_a]^{-1}$ at five different annealing temperatures. The intersection of those five curves is at 535.6 K.

that the melting peak temperature, T_m(p), and the end of melting, T_m(e), rise with increasing the annealing time, t_a,

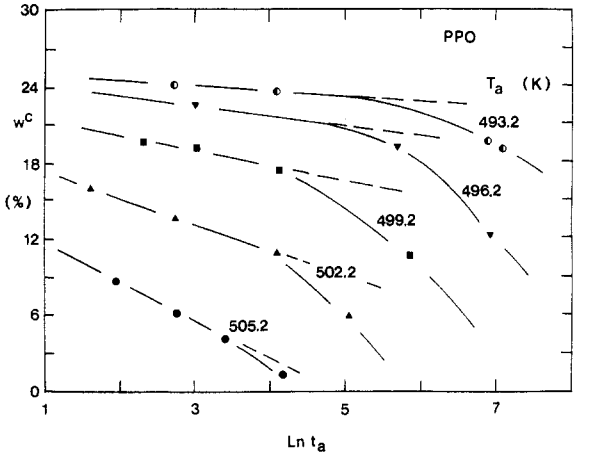

Figure 13. Relationship between crystallinity (w^c) and the logarithm of annealing time at different annealing temperatures. (See also Figures 6–10.)

at all five annealing temperatures. A linear relationship exists between T_m(p) or T_m(e) vs. the reciprocal of the logarithm of the annealing time, t_a, and is shown in Figures 11 and 12. From both figures, one can also observe that at the same annealing temperature, the slopes of both extrapolations for T_m(p) and T_m(e) are very similar, i.e., the width of melting peaks does not change (about 7.6 K).

Fusion of Semicrystalline PPO. From Figures 6–10 it can be observed that with increasing length of annealing, the heat of fusion *decreases*. The crystallinities are listed in Table II, as well as the rigid fractions, f_r, obtained from ΔC_p information, and $f_r - w^c$, the rigid-amorphous fraction. It is clear that for higher annealing temperatures, faster crystal melting occurs; e.g., at T_a = 493.2 K, the crystals need 20 h to reach a crystallinity of 9.3% from the original w^c = 28%. However, at T_a = 505.2 K, one needs only 1 h to reach a w^c = 1.5%. Also, one can see that the rigid fraction, f_r, decreases faster than the crystallinity. The rigid-amorphous fraction, $f_r - w^c$, decreases thus also faster than the crystallinity. Figure 13 shows the relationship between crystallinity of semicrystalline PPO at different

Table II
Thermal Properties of the As-Received PPO in the Melting Transition Region Measured by Heating after Annealing for Time t_a at Temperature T_a

	T_a, K	t_a, min	w^c	T_m(p)	T_m(e)	f_r	$f_r - w^c$
A							
	493.2	0	0.280	517.0	527.0	[a]	
	493.2	15	0.242	519.8	527.5	(?)[b]	(?)
	493.2	60	0.237	522.6	530.2	(?)	(?)
	493.2	960	0.197	524.6	532.2	0.455	0.258
	493.2	1200	0.192	524.9	532.4	0.421	0.229
B							
	496.2	20	0.226	521.7	529.2	0.602	0.376
	496.2	300	0.193	524.5	532.1	0.421	0.228
	496.2	990	0.122	525.1	532.7	0.303	0.181
C							
	499.2	10	0.196	520.8	528.4	0.518	0.322
	499.2	20	0.190	522.5	530.1	0.475	0.285
	499.2	60	0.174	523.8	531.3	0.420	0.246
	499.2	330	0.120	525.0	532.6	0.295	0.175
D							
	502.2	5	0.165	520.0	527.6	0.438	0.245
	502.2	15	0.136	522.5	530.0	0.344	0.208
	502.2	60	0.111	524.4	532.0	0.281	0.170
	502.2	150	0.060	525.0	532.6	0.219	0.135
E							
	505.2	7	0.086	520.8	528.3	0.188	0.102
	505.2	15	0.062	523.1	530.7	0.154	0.092
	505.2	30	0.042	524.0	531.6	0.125	0.083
	505.2	65	0.015	525.0	532.6	0.082	0.067

[a] ΔC_P is too small to be determined; f_r approaches 1.0. [b] (?) = see Table I.

annealing temperatures and the logarithm of the annealing time. Linear relationships satisfy the shorter annealing times. With increasing t_a, the crystallinity decreases faster than given by the straight lines.

Discussion

Heat Capacities. The heat capacities recommended for solid and liquid PPO were shown to be reliable to perhaps better than 1%. This means it will also be possible to derive the integral thermodynamic functions enthalpy, entropy, and Gibbs free energy for different PPO samples.[26] At present, the heat capacities serve as a "base line" for more precise thermal analysis of the amorphous and semicrystalline polymers (ATHAS).[27]

Between the glass transition and the beginning of melting one expects, in the framework of the two-phase crystallinity model, that the overall heat capacity is

$$C_p = w^c C_p(s) + (1 - w^c) C_p(l) \quad (5)$$

Some polymers, such as polyethylene,[28] follow eq 5 very closely, indeed. A negative deviation from eq 5 is interpreted by us as the existence of a "rigid-amorphous fraction". It refers to parts of the polymer that do not contribute to the heat of fusion (out of which the crystallinity, w^c, is computed) and, also, do not give rise to a contribution to the increase in heat capacity on devitrification (i.e., it refers to a part of the polymer that is not crystalline but retains above T_g the solid heat capacity that consists of vibrational contributions only). Other polymers that can have a rigid-amorphous fraction when semicrystalline are poly(oxymethylene),[25] polypropylene,[29] PEEK,[22] and PPS.[23] In case of polypropylene, the rigid-amorphous fraction unfroze continuously over a wide temperature range.[29] In case of poly(oxymethylene) no change in the rigid-amorphous fraction was observed up to melting.[25] In the more rigid, phenylene-containing polymers, the rigid-amorphous fraction depended on the crystallization annealing conditions.[22,23] In PEEK it was, for example, possible to decrease the rigid-amorphous fraction to practically zero by high-temperature crystallization or annealing with an increase in crystallinity.[22] Rigid-amorphous PPO behaves differently, as will be discussed below.

The lower heat capacity of the as-received sample (Figure 1) *below* T_g was originally attributed to some additional crystallization contributing an exotherm. The total amount of crystallinity would have to be relatively small (4% in our example). Crystallization below the glass transition is, however, a rare occurrence. It seems particularly unlikely since annealing at just slightly higher temperature actually substantially reduces crystallinity (see below). A more likely explanation is a release of strain in the, at that temperature, glassy amorphous PPO. Such size exotherms were observed before on heating of quenched amorphous,[30] and finely divided[31] polystyrenes cooled under pressure.[32] The value of 2 J/g that corresponds to 240 J/mol is typical for strain release.

Glass Transition and Hysteresis Effect. Table I and Figures 2 and 6–10 show that amorphous PPO has the sharpest and largest glass transition. The observed ΔC_p of 32 J/(K mol) from eq 3 and 4 is larger than expected for "one-bead" polymers.[27] The increase in ΔC_p in going from polyethylene (CH_2-bead) to poly(oxy-1,4-phenylene) (O-C_6H_4-bead) to the present PPO from 10.5 to 21.4 to 32 J/(K mol), respectively, is a measure of the size and mobility increase of the bead.

For semicrystalline PPO, the glass transition range is shifted and broadened to higher temperature (maximum shift observed 12 K at 10 K/min heating rate). The shorter the annealing time, and the lower the annealing temperature (the higher the crystallinity), the larger is the shift in T_g and the broadening of the transition. Coupled with this broadening of the glass transition range to higher temperatures is an increase in the amount of rigid-amorphous PPO (Table II).

When the annealing time is short enough, and the annealing temperature is low enough, almost no glass transition region can be observed at all; i.e., practically all of the amorphous portion becomes rigid.

Figures 2 and 3 show that amorphous PPO has a typical hysteresis behavior of the heat capacity in the glass transition region when a slowly cooled sample is heated

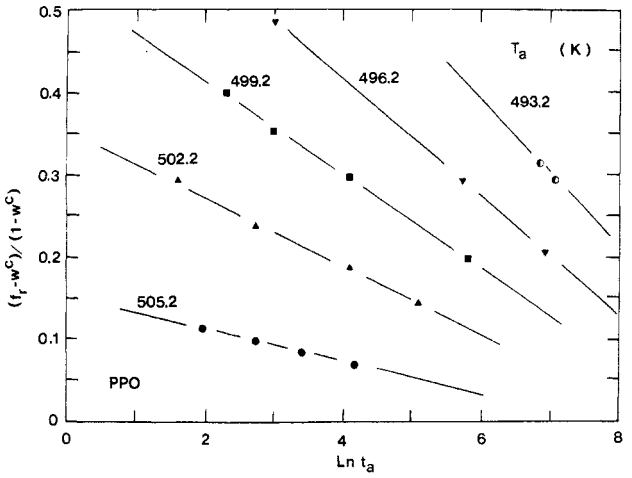

Figure 14. Relationship between $(f_r - w^c)/(1 - w^c)$ and the logarithm of annealing time at different annealing temperatures. (See also Figures 6–10.)

quickly.[30] As long as the cooling rate is slower than 2.5 K/min, the hysteresis effect of PPO is similar to that observed for other polymers;[22-23,27,30,32] i.e., a linear relationship exists between Δh of the hysteresis peak and the logarithm of the cooling rate, $\Delta h = 0$ being extrapolated to the condition that heating and cooling rates are about equal (10 K/min).

The positive deviation from the straight line in Figure 3 indicates that the freezing and unfreezing of motion of PPO at the glass transition temperature is largely asymmetric. To a much smaller degree, such asymmetry can also be noted, for example, in polystyrene that will always show a small hysteresis peak on equal cooling and heating through T_g.[30] As an explanation of this effect, one can imagine that annealing is still possible on cooling during the short time the sample is traversing the temperatures just below T_g. No such annealing occurs on the sometimes even slower heating since that would be registered as an exotherm. With symmetric relaxation times, ideally, a small exotherm below and a similar size endotherm above T_g are expected for equal cooling and heating rates.[30]

The influence of rigid polymer (crystalline and rigid amorphous) on the hysteresis is more than the numerical mass fraction (see Figure 4). A larger number of other crystalline polymers behaved similarly.[33] Broadening of the transition region, as is documented in Table I, alone cannot be a reason for the complete absence of hysteresis above about 50% rigid PPO. A full explanation is presently not available.

The decrease in rigid fraction with annealing temperature and time as measured by the increase in ΔC_p of Figure 5 (see also Tables I and II) is rather surprising. If the process were caused by fusion followed or accompanied by crystal perfection, one would not have a long-time continuous increase in amorphous PPO, but rather a quick production of the amorphous, followed by a slow increase of crystallinity.

Annealing and Fusion of Semicrystalline PPO. A look at Figures 6–10 shows that annealing below the major melting peak of the initial semicrystalline sample causes (1) a reduction in rigid amorphous (strain release), (2) a reduction in crystallinity (fusion), and (3) an increase in perfection of the remaining crystals (annealing) indicated by a shift in melting peak (without broadening) (see Table II). Effect 3 is well illustrated by Figures 11 and 12. These figures also seem to suggest that the best crystals obtainable by this procedure with a T_m(p) of 528 K and a T_m(e) of 535.6 K would still be far from equilibrium perfection (T_m = 580 K) and be produced only in infinitesimal amounts.

The slow decrease in crystallinity cannot be linked to typical superheating of large crystals since this should have an exponential time dependence[21] (see Figure 13). Instead, the slow melting seems to be exponentially proportional to the total rigid-amorphous fraction in the overall amorphous part of the polymer, as illustrated in Figure 14. If the ratio of rigid-amorphous fraction to crystallinity is computed, 15 measurements from all different T_a and t_a give a constant value of 1.5 ± 0.2. All of this points to the complexity of relaxation of the rigid-amorphous PPO and melting and annealing.

Without rigid-amorphous fraction, one would expect crystals of the small size of PPO crystals to melt practically instantaneously. Without annealing and without rigid-amorphous fraction to retard melting one would guess that the melting peak of the as-received sample (Figure 1) is at an even lower temperature. The major melting could be expected to be completed at 500 K.

Conclusions

The special properties of semicrystalline PPO have been linked to the existence of a rigid-amorphous phase which governs the thermal properties from T_g to T_m. Fusion, superheating, and annealing are directly linked to the rigid-amorphous fraction. One expects a similar or even greater effect on the mechanical and dielectric properties.

The negative C_p defect below T_g for semicrystalline PPO is more likely a stress relaxation rather than additional crystallization.

The amorphous PPO also has some special relaxation behavior at the glass transition pointing to an especially large asymmetry of relaxation on cooling and heating. The well-known absence of brittleness below T_g has no indication of a thermally detectable transition. Below T_g the heat capacities reach quickly the level calculated from a pure vibration.

Acknowledgment. This research was supported by the National Science Foundation, Polymers Program, Grant DMR 83-17097.

References and Notes

(1) Hay, A. S.; Blanchard, H. S.; Endres, G. F.; Eustance, J. W. *J. Am. Chem. Soc.* **1959**, *81*, 6335.
(2) Hay, A. S.; Shenian, P.; Growan, A. C.; Erhardt, P. F.; Haaf, W. R.; Therbege, S. E. *Encyclopedia of Polymer Science and Technology*, Interscience: New York, 1969; Vol. 10, p 92.
(3) Karasz, F. E.; Bair, H. E.; O'Reilly, J. M. *J. Polym. Sci., Part A-2* **1968**, *6*, 1141.
(4) Cheng, S. Z. D.; Lim, S.; Judovits, L.; Wunderlich, B. *Polymer* **1987**, *28*, 10.
(5) Gaur, U.; Wunderlich, B. *J. Phys. Chem. Ref. Data* **1981**, *10*, 1001.
(6) Jauhiainen, T.-P. *Makromol. Chem.* **1982**, *104*, 107; **1982**, *183*, 925.
(7) Barrales-Rienda, J. M.; Fatou, J. M. *Kolloid Z. Z. Polym.* **1971**, *244*, 317.
(8) Packter, A.; Sharif, K. A. *J. Polym. Sci., Part B* **1971**, *9*, 435.
(9) Koenhen, D. M.; Bakker, A.; Broens, L.; van den Berg. J. W. A.; Smolders C. A. *J. Polym. Sci., Polym. Phys. Ed.* **1984**, *22*, 2145.
(10) Wenig, W.; Hammel, R.; MacKnight, W. J.; Karasz, F. E. *Macromolecules* **1976**, *9*, 253.
(11) Shultz, A. R.; McCullough, C. R. *J. Polym. Sci., Part A-2* **1969**, *7*, 1577; **1972**, *10*, 307.
(12) van Emmerik, P. T.; Smolders, C. A. *Eur. Polym. J.* **1973**, *9*, 293. See also: Janaczek, H.; Turska, E.; Szekely, T.; Leugyuel, M. *Polymer* **1978**, *19*, 85.
(13) Hammel, R.; MacKnight, W. J.; Karasz, F. E. *J. Appl. Phys.* **1975**, *46*, 4199.
(14) Wenig, W.; Karasz, F. E.; MacKnight, W. J. *J. Appl. Phys.* **1975**, *46*, 4194.
(15) Berghmans, H.; Overbergh, N. *J. Polym. Sci., Polym. Phys. Ed.* **1977**, *15*, 1757.

(16) Wenig, W.; MacKnight, W. J.; Karasz, F. E. *Macromolecules* **1986**, *19*, 1272.
(17) Hobbs, S. Y. *Bull. Am. Phys. Soc.* **1986**, *31*(3), 460.
(18) Bopp, R. C.; Gaur, U.; Kambour, R. P.; Wunderlich, B. *J. Thermal Anal.* **1982**, *25*, 243; unpublished results.
(19) Jauhiainen, T.-P. *Makromol. Chem.* **1982**, *104*, 117.
(20) Koenhen, D. M.; Smolders, C. A. *J. Polym. Sci., Polym. Phys. Ed.* **1977**, *15*, 155; **1977**, *15*, 167. Koenhen, D. M.; Smolders, C. A. *J. Polym. Sci., Polym. Symp.* **1978**, *61*, 93.
(21) For a review, see: Wunderlich, B. *Macromolecular Physics*; Academic: New York, 1980; Vol. III, Crystal Melting.
(22) Cheng, S. Z. D.; Cao, M.-Y.; Wunderlich, B. *Macromolecules* **1986**, *19*, 1868.
(23) Cheng, S. Z. D.; Wu, Z. Q.; Wunderlich, B. submitted for publication in *Macromolecules*.
(24) Wunderlich, B.; Bopp, R. C. *J. Thermal. Anal.* **1974**, *6*, 335. See also: Mehta, A.; Bopp, R. C.; Gaur, U.; Wunderlich, B. *J. Thermal Anal.* **1978**, *13*, 197.
(25) Suzuki, H.; Grebowicz, J.; Wunderlich, B. *Makromol. Chem.* **1985**, *189*, 1109.
(26) Cheng, S. Z. D.; Wunderlich, B., unpublished results.
(27) Wunderlich, B.; Cheng, S. Z. D. *Gazz. Chim. Ital.* **1986**, *116*, 345.
(28) Wunderlich, B. *J. Chem. Phys.* **1962**, *37*, 1203; *J. Polymer Sci., Part C* **1963**, *1*, 41. Gaur, U.; Wunderlich, B. *J. Phys. Chem. Ref. Data* **1981**, *10*, 119.
(29) Grebowicz, J.; Lau, S. F.; Wunderlich, B. *J. Polym. Sci., Polym. Symp.* **1984**, *71*, 19.
(30) Wunderlich, B.; Bodily, D. M.; Kaplan, M. H. *J. Appl. Phys.* **1964**, *35*, 95.
(31) Gaur, U.; Wunderlich, B. *Macromolecules* **1980**, *13*, 1618.
(32) Weitz, A.; Wunderlich, B. *J. Polym. Sci., Polymer Phys. Ed.* **1974**, *12*, 2473.
(33) Menczel, J.; Wunderlich, B. *J. Polymer Sci., Polym. Lett.* **1981**, *19*, 261.

Influence of a Functional Group Situated along the Side Chain on Side-Chain Crystallinity and on the Heat and Entropy of Melting of Comblike Poly[*N*-((*n*-alkyl(oxycarbonyl))methyl)maleimides] and Poly[*N*-(5-(*n*-alkyl(oxycarbonyl))-*n*-pentyl)maleimides]

José M. Barrales-Rienda* and José M. Mazón-Arechederra

Instituto de Plásticos y Caucho, Consejo Superior de Investigaciones Científicas, Juan de la Cierva, 3, 28006 Madrid, Spain. *Received August 6, 1986*

ABSTRACT: Thermodynamic properties of poly[*N*-((*n*-alkyl(oxycarbonyl))methyl)maleimides] (PEMIs 1) containing 14–22 carbon atoms and poly[*N*-(5-(*n*-alkyl(oxycarbonyl))-*n*-pentyl)maleimides] (PEMIs 5) containing 12–22 carbon atoms, in the outer part of the lateral *n*-alkyl side chain were studied by means of differential scanning calorimetry and a refractometric technique. The influence of an ester group situated along the lateral *n*-alkyl side chain on the crystallization of the side chains was studied. The thermal properties of these two homologous series of comblike polymers were compared to those of poly[*N*-(10-(*n*-alkyl(oxycarbonyl))-*n*-decyl)maleimides] (PEMIs 10) because of strong similarities in properties and structure. The enthalpic data for these three series (PEMIs 1, PEMIs 5, and PEMIs 10) show that only a part of the outer *n*-alkyl side chain is present in the crystallization. The thermal properties and thermodynamic characteristics appear to be adequately described by a basic model similar to that for the PEMIs 10 series. The contributions to the heat and entropy of melting per methylene group show that the hexagonal paraffinlike crystal modification is present in the PEMIs 1 and PEMIs 5 series, in good agreement with X-ray diffraction data for the same compounds. There exist for the three homologous series good linear correlations between the critical chain length in the outer part of the *n*-alkyl side chain needed to initiate the crystallization and the term $\Delta H_{t,e}$ due to the chain-end contribution to the melting enthalpy.

Introduction

This article discusses the results of an extension to PEMIs 1 and PEMIs 5 of a previous calorimetric study of PEMIs 10.

It has been well established that polymers with long *n*-alkyl side chains crystallize. Only in a few cases has a quantitative determination of the degree of crystallinity of these comblike polymers been made. Some authors have measured the heat of melting, the melting temperatures, the derived entropies of melting and, in a few cases, the degree of crystallinity. Dependence of the thermodynamic properties and/or degree of crystallinity on *n*-alkyl side chain length has been examined for atactic poly(1-alkyl acrylates),[1] poly(1-alkyl acrylamides),[2] poly(1-alkyl vinyl esters),[1,2] poly(1-alkyl methacrylates),[3,4] poly(di-*n*-alkyl itaconates),[5] poly[*N*-(*n*-alkyl)maleimides],[6] poly[*N*-(10-(*n*-alkyl(oxycarbonyl))-*n*-decyl)maleimides][7] (PEMIs 10), stereoregular and atactic poly(1-alkylethylenes),[8,9,10] stereoregular and atactic poly(1-alkylethylene oxides),[10,11] and poly(γ-*n*-alkyl L-glutamates).[12] Almost all authors have reached the conclusion that the part of the *n*-alkyl side chain extending beyond eight methylene groups participates in the crystallization.

It was of interest to study the influence of a functional group situated along the *n*-alkyl side chain on the crystallinity and thermodynamic properties of comblike polymers with long *n*-alkyl side chains. Consequently, a study of the homologous series of PEMIs 1 and PEMIs 5 was undertaken. They have one and five methylene groups in the inner part of the *n*-alkyl side chain, respectively.

There are two fundamental aspects to the present work: (1) to show the influence of the length of the outer part of the *n*-alkyl side chain within each of the two homologous series of PEMIs 1 and PEMIs 5 independently on the crystallization and heat and enthalpy of melting and (2) to discover the role played by the functional group situated along the *n*-alkyl side chain or the inner part of the *n*-alkyl side chain of the three homologous series of PEMIs 1, PEMIs 5, and PEMIs 10 on the estimated values of some characteristic thermodynamic parameters.

The structural unit of the comblike polymers that will be studied in the present paper may be represented by the simplified chemical structure given in Figure 1.

Our three homologous series of comblike polymers, PEMIs 1, PEMIs 5, and PEMIs 10, have as a main feature an ester group situated along the *n*-alkyl side chain. Be-

0024-9297/87/2220-1637$01.50/0